Journal of the Nivar Volume 50, Special Issue, Spring and Summer 2026, P. 01-20
Homepage: https://nivar.irimo.ir (Research Article)

Decoding the Direction and Magnitude of Wind Speed Trends Using Multiple Statistical Approaches

Hedieh Ahmadpari [1] | **Vitaly Khaustov** [2] | **Hamed Abbasali Nezhad** [3]

[1] PhD candidate, Hydrology of land, water resources, hydrochemistry, Department of Engineering Hydrology, Institute of Hydrology and Oceanology, Russian State Hydrometeorological University, Saint Petersburg, Russia.
[2] Candidate of Technical Sciences, Associate Professor, Department of Engineering Hydrology, Institute of Hydrology and Oceanology, Russian State Hydrometeorological University, Saint Petersburg, Russia.
[3] M.Sc. in Applied Meteorology; Secretary of Agricultural Meteorology Development, West Azerbaijan Province, and Head of the Agricultural Meteorology Research Station, Urmia University, Urmia, Iran.

Corresponding Author E-mail: h-alinezhad@irimo.ir

(Received: 04 Nov 2025, Revised: 06 Jun 2026, Accepted: 10 Jun 2026, Published online: 10 Jun 2026)

Abstract

Analyzing wind speed trends provides valuable insights into regional climate dynamics, atmospheric circulation changes, and their impacts on environmental and energy systems. This study investigates the temporal trends of monthly and annual wind speed in the Darreh Dozdan River basin, located in Lorestan Province, Iran, using a 25-year dataset (1998–2022) from the Kuhdasht synoptic station. Both parametric (linear regression and Pearson correlation coefficient) and nonparametric (Mann–Kendall test and Sen's slope estimator) methods were applied to detect and quantify wind speed trends. The Mann–Kendall test showed that all months had positive and statistically significant Z values greater than +1.96, confirming a persistent upward trend in wind speed. The strongest increases occurred in June, August, and September (Z = 4.27–4.86), reflecting intensified wind activity during the warmer months. The Sen's slope and linear regression analyses revealed the largest increases in wind speed during February (0.12 m/s per year) and March (0.14 m/s per year), indicating that wind speeds rose most rapidly in late winter and early spring, while the annual results from both methods confirmed a steady increase in average wind speed of 0.08 m/s per year. Pearson correlation coefficients showed significant positive relationships ($r > 0.6$ for all months), with the strongest correlations in June, August, and September ($r > 0.8$), confirming a highly consistent and stable upward trend during these months. All four analytical methods converged on the conclusion that wind speed had increased in a statistically significant and persistent manner, differing only in which months exhibited the steepest or most stable growth, thereby providing a comprehensive and robust confirmation of wind intensification in the Darreh Dozdan River basin. These findings highlight the importance of accounting for increasing wind intensity in future regional climate assessments, water resource management, and land-use planning within the basin.

Keywords: Wind speed trend, Mann–Kendall test, Sen's slope estimator, Pearson correlation, Linear regression

1. Introduction

Climate change refers to alterations in typical weather patterns at both local and global scales (Kara and Şahin, 2023). Primarily driven by the enhanced greenhouse effect, it has profoundly altered the Earth's atmospheric energy balance and circulation systems (Kleidon et al., 2023). As concentrations of greenhouse gases such as carbon dioxide, methane, and nitrous oxide continue to rise, global temperatures increase, leading to shifts in large-scale pressure gradients and atmospheric dynamics (Zhang et al., 2021). These changes influence major atmospheric circulation systems, including the Hadley, Ferrel, and Walker cells, directly affecting regional wind patterns and intensities.

Cite this article: Abasalinezhad,H , Ahmadpari,H and Khaustov,V . (2026). Decoding the Direction and Magnitude of Wind Speed Trends Using Multiple Statistical Approaches. Journal of the Nivar, Special Issue, 01-20. DOI: https://doi.org/10.30467/nivar.2026.557484.1358

E-mail: (1) h.ahmadpari@stud.rshu.ru (2) vitaly.khaustov3@mail.ru

Publisher: Iran Meteorological Organization
DOI: https://doi.org/10.30467/nivar.2026.557484.1358
Print ISSN: 1735-0565
Online ISSN: 2645-3347

Recent studies show that climate warming can cause both strengthening and weakening of wind regimes depending on geographic and topographic conditions. Such alterations impact energy and moisture transport, with consequences for weather systems, renewable energy resources, and agricultural processes (Park et al., 2024; Wang et al., 2024).

Wind, defined as the horizontal movement of air due to differences in atmospheric pressure caused by uneven solar heating, plays a fundamental role in regulating the climate system (Kara and Şahin, 2023; Berna-Escriche et al., 2025). It redistributes heat, moisture, and pollutants, influences cloud formation and precipitation, and helps maintain the global energy balance between the equator and poles. Beyond its climatic function, wind is critical for environmental and socio-economic processes, including air quality management, renewable energy generation, and agricultural productivity (Rasheed and Ullah, 2023).

Food security, defined as access to sufficient, safe, and nutritious food for all individuals to live a healthy life (FAO, 2023), is directly threatened by climate change (IPCC, 2022). Rising temperatures, altered precipitation patterns, and increased extreme weather events such as droughts, floods, and storms undermine agricultural productivity (Rahman et al., 2022; Tanikawa & Hashimoto, 2022). These impacts reduce crop yields, increase plant diseases and pests, and limit water availability for agriculture, particularly affecting developing countries and vulnerable populations (Owasa & Fall, 2024; Smith et al., 2022).

Wind also significantly influences agricultural and hydrological processes. It affects evapotranspiration by enhancing moisture transfer from soil and plants to the atmosphere, thereby influencing soil moisture, crop water use, and productivity (Wanniarachchi & Sarukkalige, 2022; Fu et al., 2022). Changes in wind speed can alter crop water demand, affecting irrigation strategies and food production (Mincu et al., 2025). Additionally, wind impacts crop pollination, evapotranspiration rates, and soil erosion (Balfour & Ratnieks, 2025; Markwitz et al., 2020; Qin et al., 2025).

To identify trends in wind speed over time, researchers employ parametric and non-parametric statistical methods. Parametric approaches, assuming specific data distributions, include linear regression and Pearson's correlation coefficient (Akçay et al., 2022; Mirabbasi et al., 2020; Yılmaz & Kara, 2024). Non-parametric methods, including the Mann–Kendall trend test and Sen's slope estimator, are more robust against non-normality and extreme values (Gutiérrez Hernández et al., 2024). Combining both approaches provides a more comprehensive assessment of wind speed trends (Akçay et al., 2022; Aschale et al., 2023).

A growing body of observational and reanalysis-based research has examined global and regional changes in wind speed. Deng et al. (2021) reported overall weakening over land surfaces but slight strengthening in some marine regions. Hahmann et al. (2022) found that mean wind speeds and wind power densities in parts of the North Sea may not change substantially in the annual mean between 2031–2050 compared to 1995–2014, though seasonal shifts are expected to affect summer energy production. Zhao et al. (2023) and Shi et al. (2022) emphasize that interpreting heterogeneous wind trends requires accounting for local factors such as topography, coastal versus inland location, measurement height, and regional circulation shifts. Siddiqui et al. (2025) reported significant reductions in near-surface wind speeds and wind energy potential under high-warming scenarios across the Middle East and North Africa. Understanding spatial and temporal wind variability is essential for distinguishing long-term trends from short-term fluctuations.

Despite numerous studies on wind speed trends, many rely solely on parametric or non-parametric methods, potentially introducing biases or overlooking subtle variations (Totaro et al., 2020). Moreover, global or regional analyses may obscure localized dynamics crucial for water management, agriculture, and climate adaptation. To address these gaps, focused studies on specific basins or regions are essential. Such localized analyses provide detailed understanding of wind behavior, its interactions with topography, vegetation, and microclimate, and yield actionable insights for sustainable agriculture, water resource planning, and climate-resilient policy development (Luo et al., 2022).

The Darreh Dozdan River basin, located in Lorestan Province, Iran, is a climatically sensitive region where wind dynamics influence local weather patterns, evapotranspiration, and land degradation.

Despite its environmental and agricultural importance, no previous studies have investigated wind speed trends in this basin. Assessing the temporal behavior of wind speed is crucial for understanding regional climate variability and its potential impacts on water resources, agriculture, and soil conservation. Therefore, the main objective of this study is to analyze monthly and annual trends in wind speed in the Darreh Dozdan River basin using both parametric and nonparametric statistical methods. The findings are expected to fill an important research gap and provide a scientific basis for future climate adaptation and resource management strategies in the region.

2.Materials and methods

2.1. Study area

The Darreh Dozdan River basin is located in Lorestan Province, Iran. It is part of the second-level watershed known as the Karkheh basin (Ahmadpari and Khaustov, 2025a). In this study, to analyze wind speed trends in the Darreh Dozdan River basin, data from the Kuhdasht synoptic station were utilized. The Kuhdasht synoptic station has been established and operated by the Iran Meteorological Organization since 1997. It is situated at 47°38′52″E longitude, 33°31′27″N latitude, and an elevation of 1,197 meters above sea level (Ahmadpari and Khaustov, 2025b). Figure 1 shows the geographic location of the study area within Lorestan Province and Iran.

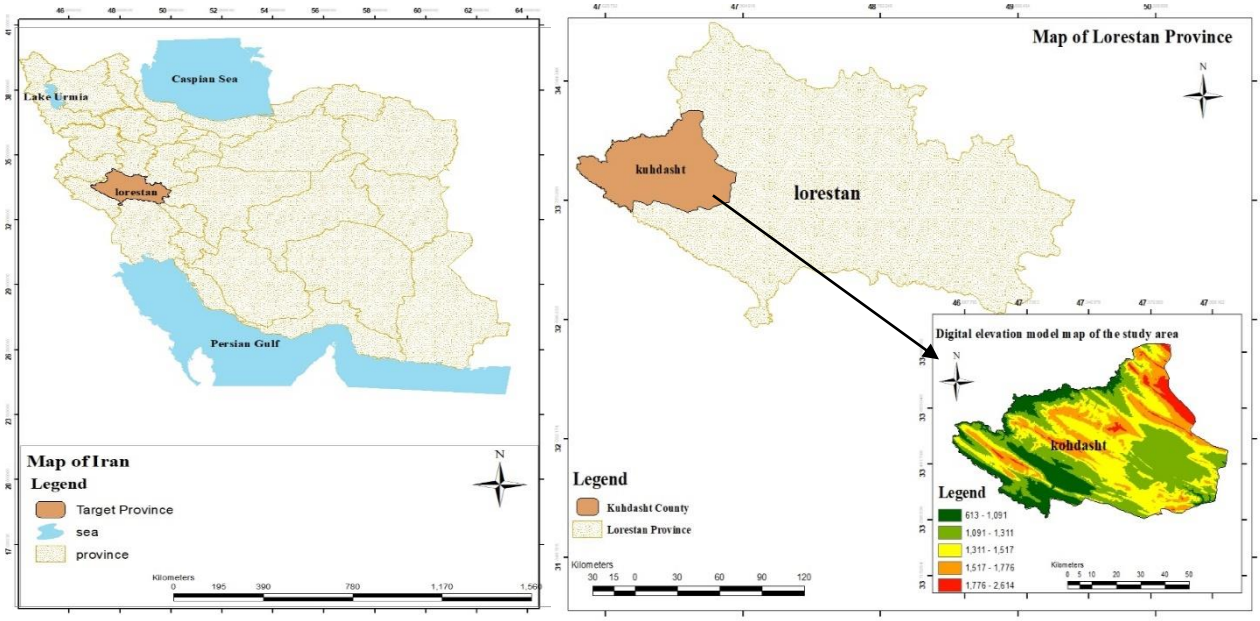

Figure 1. Geographical location of the study area

2.2. Monthly and annual wind speed trends

spanning 25 years from 1998 to 2022, were collected for analysis. The trends were assessed using both parametric methods, including regression analysis and Pearson correlation, and non-parametric methods, specifically the Mann–Kendall test and Sen's slope estimator. The Mann–Kendall and Sen's slope computations were performed using the MAKESENS 1.0 Excel macro, a freeware released by the Finnish Meteorological Institute in 2002. Mann–Kendall plots were generated using the Mann–Kendall Excel macro, developed in 2017 by the Iran Meteorological Organization. Regression analyses and Pearson correlation coefficients were calculated using Microsoft Excel 2019. A 95% confidence level was used to assess statistical significance, with p-values below 0.05 considered significant and those above 0.05 not significant (Kwak, 2023).

2.2.1. Mann-Kendall test

The Mann–Kendall test is a widely applied nonparametric method for identifying monotonic trends, whether increasing or decreasing, in hydrological and climatic time series, without assuming any specific underlying data distribution (Liu et al., 2022). In the Mann–Kendall test, the null hypothesis states that no trend is present, whereas the alternative hypothesis indicates the existence of

a monotonic trend, either upward or downward, throughout the study period (Afrazfar et al., 2025). The Mann–Kendall test has proven particularly effective in environmental and climatological analyses (Totaro et al., 2020), especially for wind speed time series, as it is robust to non-normal distributions and insensitive to abrupt changes or breaks in the data (Ahmadpari et al., 2025). The S statistic of the Mann–Kendall test, which represents the cumulative difference between each observation and all subsequent observations, was calculated using Equation 1 (Ahmadpari et al., 2025).

$$S = \sum_{i=1}^{n-1} \sum_{j=i+1}^{n} \operatorname{sgn}(x_j - x_i) \quad (1)$$

In this relation, n is the number of observations in the series; x_j and x_i are the jth and ith data of the series, respectively. The sgn function is calculated with Equation 2 (Thenmozhi and Kottiswaran, 2016).

$$\operatorname{sgn}(x) = \begin{bmatrix} +1 & (x_j - x_i) > 0 \\ 0 & (x_j - x_i) = 0 \\ -1 & (x_j - x_i) < 0 \end{bmatrix} \quad (2)$$

The variance of S is determined using Equation 3 (Hejazizadeh et al., 2022).

$$\operatorname{var}(S) = \frac{n(n-1)(2n+5)}{18} \quad (3)$$

Also, the standardized Z statistic is calculated using Equation 4 (Hejazizadeh et al., 2022).

$$Z = \begin{cases} \frac{S-1}{\sqrt{\operatorname{Var}(S)}} & \text{if } S > 0 \\ 0 & \text{if } S = 0 \\ \frac{S+1}{\sqrt{\operatorname{Var}(S)}} & \text{if } S < 0 \end{cases} \quad (4)$$

The null hypothesis is accepted if $|Z| \leq Z_{\frac{\alpha}{2}}$ at the α level of significance in a two-sided test for trend (Chen et al., 2016). If Z is positive, the trend of the data series is considered upward, and if it is negative, the trend is considered downward (Chen et al., 2016). If the Z value lies between -1.96 and +1.96, the trend in the time series is not statistically significant at the 0.05 confidence level. When the Z value exceeds +1.96, the time series trend is significantly increasing. Conversely, if the Z value is less than -1.96, the trend is significantly decreasing (Nguyen et al., 2022). The Mann-Kendall Jump Test, also known as the sequential Mann-Kendall test or the Mann-Kendall Change Point Test, is a statistical method for detecting abrupt changes in time series data. It is an extension of the general Mann-Kendall trend test, which assesses the overall direction of change, whether increasing or decreasing, in a time series. The purpose of the Jump Test is to identify the specific points in time where a statistically significant change in the trend occurs (Mokari and Abbasnia, 2020). The Mann-Kendall Jump Test involves calculating two series of statistics: a "forward" (U_i) series and a "backward" (U_i') series. The 'i' represents the time point in the series. The method of U_i series and U_i' series calculations with all its formulas is described in the study by Liu and Xu (2016). A potential jump point, also known as a change point, is identified at the intersection of the two lines. For this intersection to be considered a statistically significant jump, it must occur beyond the critical value boundaries, which are set at ±1.96 (Amiri et al., 2015). Multiple intersections may occur, indicating the presence of several jump points. When the lines representing U_i and U_i' intersect beyond the critical value boundaries, this indicates a statistically significant change in the trend at that time. The intersection point corresponds to the estimated jump point. The direction of the jump can be deduced by analyzing the behavior of the U_i line before and after the intersection. For instance, if U_i is positive prior to the intersection and negative afterwards, this signifies a shift from an increasing trend to a decreasing trend, or vice versa. If no intersections occur outside the critical thresholds, then no statistically significant jump points are detected (Ahmadpari et al., 2025).

2.2.2. Sen's Slope Estimator

The Sen's slope estimator is commonly used to detect linear trends in time series data (Afrazfar et al., 2025). The method is based on calculating the median slope of the time series and evaluating its linearity at different confidence levels. Sen's slope has an advantage over linear regression because it is less affected by outliers

and data inaccuracies (Afrazfar et al., 2025). For N pairs of data points in the time series, the slope between these two points was calculated using Equation 5 (Keskin et al., 2025).

$$Q_i = \frac{x_j - x_k}{j - k} \quad \text{for i} = 1, \ldots, \text{N} \qquad (5)$$

where x_j and x_k are the data values at times j and k ($j > k$), respectively. If there is only one datum in each time period, then $N = \frac{n(n-1)}{2}$, where n is the number of time periods. If there are multiple observations in one or more time periods, then $N < \frac{n(n-1)}{2}$, where n is the total number of observations (Gocic and Trajkovic, 2013). The N values of Q_i are ranked from smallest to largest, and the median of the slope or Sen's slope estimator is computed using Equation 6 (Afrazfar et al., 2025).

$$\mathrm{Q_{med}} = \begin{cases} \mathrm{Q}_{\left(\frac{\mathrm{N}+1}{2}\right)} & \text{if N is odd} \\ \dfrac{\mathrm{Q}_{\left(\frac{\mathrm{N}}{2}\right)} + \mathrm{Q}_{\left(\frac{\mathrm{N}+2}{2}\right)}}{2}, & \text{if N is even} \end{cases} \qquad (6)$$

The sign of Q_{med} indicates the direction of the data trend, while its magnitude represents the steepness of the trend. To determine whether the median slope is statistically significantly different from zero, the confidence interval of Q_{med} should be calculated at a specified confidence level. This confidence interval for the time slope can be computed using Equation 7 and Equation 8 (Gocic and Trajkovic, 2013).

$$\mathrm{Var\ (s)} = \frac{\mathrm{n(n-1)(2n+5)} - \sum_{\mathrm{i=1}}^{\mathrm{m}} \mathrm{t_i(t_i-1)(2t_i+5)}}{18} \qquad (7)$$

$$\mathrm{C_\alpha} = \mathrm{Z}_{\left(1-\frac{\alpha}{2}\right)} \sqrt{\mathrm{Var\ (S)}} \qquad (8)$$

$Z_{(1-\alpha/2)}$ is obtained from the standard normal distribution table. The lower and upper limits of the confidence interval are Q_{min} and Q_{max}. The slope Q_{med} is statistically different than zero if the two limits (Q_{min} and Q_{max}) have similar sign (Ahmadpari et al., 2025).

2.2.3. Pearson correlation coefficient

The Pearson correlation coefficient, commonly denoted as r, is a statistical measure that quantifies the strength and direction of a linear relationship between two continuous variables. Its value ranges from -1 to 1. The Pearson correlation coefficient is calculated using Equation 9 (Ahmadpari et al., 2018).

$$\mathrm{Corr(X,Y)} = \frac{\mathrm{Cov(X,Y)}}{6_\mathrm{X} 6_\mathrm{Y}} \qquad (9)$$

where, X and Y are the values of two variables, σ_X is standard deviation of variable X, σ_Y is standard deviation of variable Y, Cov (X, Y) is covariance between X and Y. The comparison of the Pearson correlation coefficient and the correlation strength is shown in Table 1.

Table 1. Classification of Pearson correlation coefficient values by strength (Jiang and Sun, 2025)

Range of Correlation Coefficients	Correlation Strength
0.0–0.2	Extremely weak correlated
0.2–0.4	Weak correlated
0.4–0.6	Medium correlated
0.6–0.8	Strong correlated
0.8–1.0	Highly correlated

To test the significance of the Pearson correlation coefficient, a t-test is typically used. The test statistic (t) is calculated using the Equation 10 (Obilor and Amadi, 2018).

$$\mathrm{t} = \frac{\mathrm{r}\sqrt{\mathrm{n}-2}}{\sqrt{1-\mathrm{r}^2}} \qquad (10)$$

where, t= t-value required for the test of significance of the correlation coefficient r, n= sample size, r= the computed correlation coefficient being tested for significance. The degrees of freedom (df) for this test are equal to n-2, where n is the number of observations (Obilor and Amadi, 2018). After calculating the test statistic t and the df, the p-value must be determined. The p-value, or probability value, is a statistical measure that helps researchers assess the significance of their experimental

results. It represents the probability of obtaining the observed data, or something more extreme, assuming that the null hypothesis is true. The null hypothesis typically states that there is no effect or no difference within the context of the study. The p-value is calculated using the Equation 11 (Ahmadpari et al., 2025).

$$p - value = T.DIST.2T(ABS(t), df) \quad (11)$$

where, ABS (t)=| t |, The ABS function is used to return the absolute value of a number. The "T.DIST.2T" function returns the two-tailed probability that a t statistic is less than or equal to a specified value, based on the t-distribution. The result of the "T.DIST.2T" function is a value between 0 and 1, representing the probability. A small p-value (typically ≤ 0.05) indicates strong evidence against the null hypothesis, so the null hypothesis would be rejected. A larger p-value (> 0.05) indicates weak evidence against the null hypothesis, so the null hypothesis would fail to be rejected (Ahmadpari et al., 2025).

2.2.4. Regression analysis

To assess the temporal trend of wind speed in the Darreh Dozdan River basin, a simple linear regression method was applied. This statistical method evaluates the linear association between a single independent variable (time) and a dependent variable (wind speed). The model fits a straight line to the observed data, mathematically represented as Equation 12 (Muhlbaueret al., 2009).

$$Y = a + bX \quad (12)$$

where Y denotes the dependent variable (wind speed in the Darreh Dozdan River basin), X is the independent variable (time or year), a is the intercept, and b is the slope, representing the rate of change in wind speed over the study period. The slope parameter b provides insight into the direction and magnitude of the trend. A positive value of b indicates an increasing trend, while a negative value signals a decrease. To determine if the observed trend was statistically significant, the p-value associated with the slope coefficient was checked. A p-value below the standard threshold (typically 0.05) suggests that the trend is unlikely to have occurred by random chance, confirming its significance in the population (Ahmadpari et al., 2025). All regression analyses were conducted using the Regression feature available in the Analysis ToolPak of Microsoft Excel 2019, which computes all model estimates and significance tests efficiently for large datasets.

3. Results and Discussion

3.1. Monthly and annual wind speed trends

3.1.1. Mann-Kendall test

Figure 2 presents the results of the Mann–Kendall jump test applied to the monthly wind speed time series of the Darreh Dozdan River basin over the period 1998–2022 (25 years).

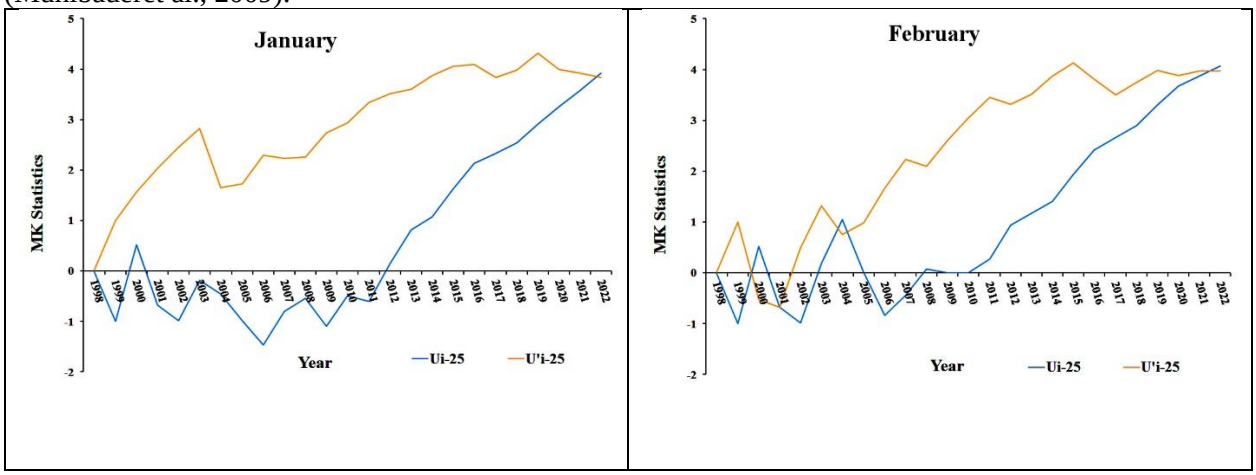

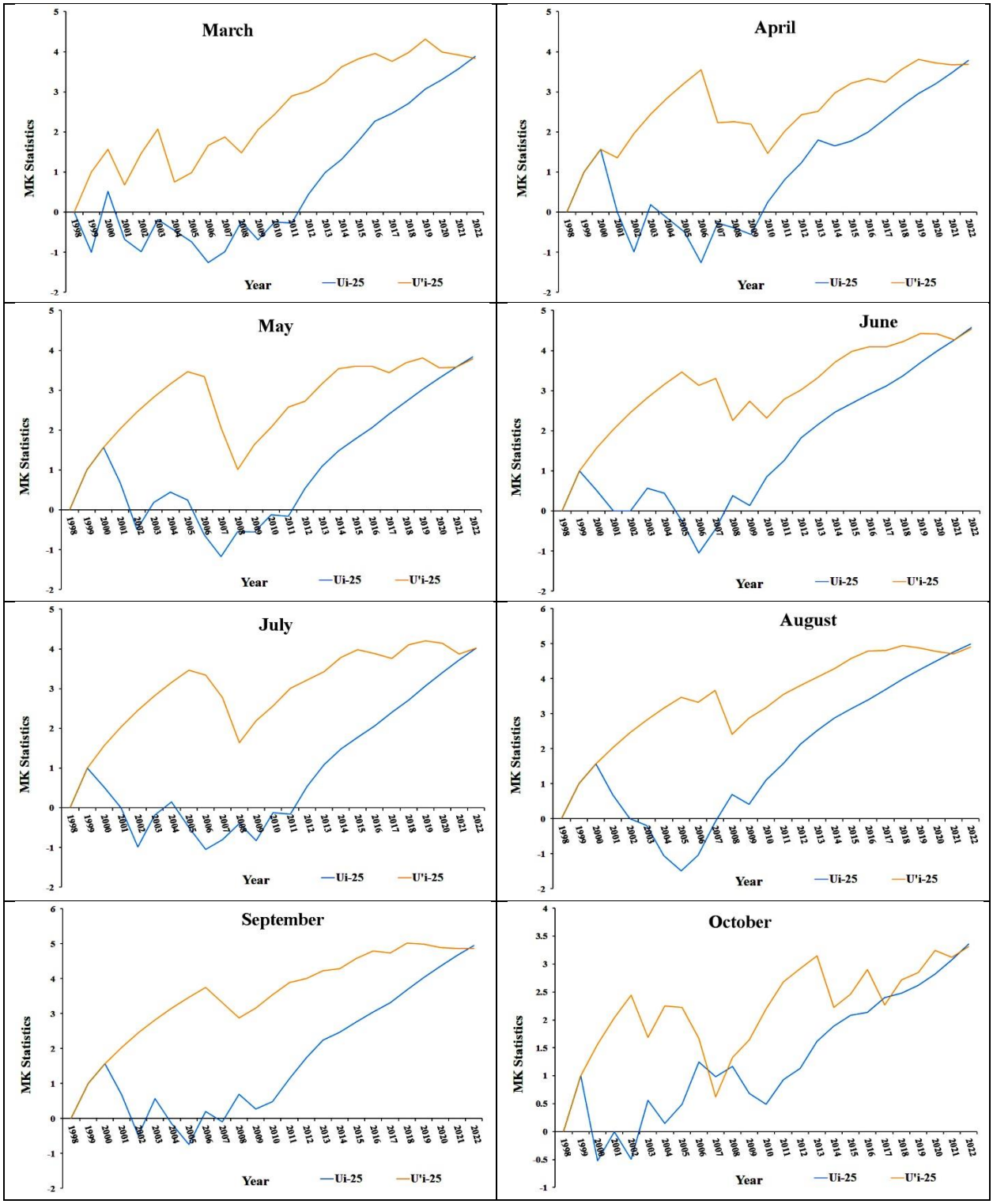
March
April
May
June
July
August
September
October
MK Statistics
Year
Ui-25
U'i-25

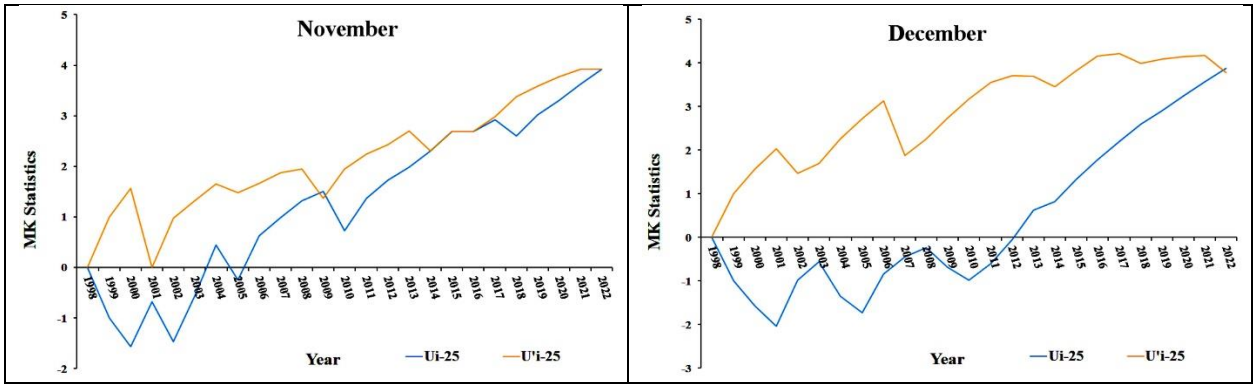

Figure 2. Mann–Kendall jump test on monthly wind speed time series data

The Mann–Kendall test results for the monthly wind speed data indicate that all months exhibit positive Z values greater than +1.96, confirming statistically significant increasing trends at the 95% confidence level. The Z values range from 3.32 in October to 4.86 in September, showing that the increase in wind speed is consistent throughout the year. The most substantial upward trends occur during summer and early autumn (June to September), while the lowest, though still significant, increase is observed in October. This consistent pattern suggests that wind speeds have intensified across all months, with stronger growth during warmer seasons. Figure 3 presents the results of the Mann–Kendall jump test applied to the annual wind speed time series of the Darreh Dozdan River basin over the period 1998–2022 (25 years).

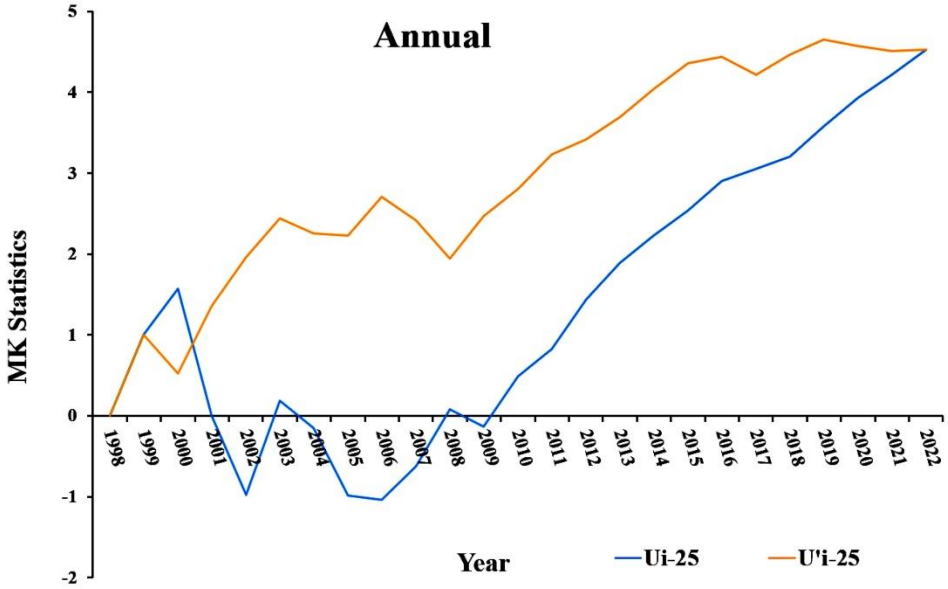

Figure 3. Mann–Kendall jump test on annual wind speed time series data

The annual Mann–Kendall Z value of 4.53 is also greater than +1.96, indicating a statistically significant upward trend in the annual average wind speed at the 95% confidence level. This result demonstrates a long-term increase in wind speed over the 25-year period from 1998 to 2022. The persistence of positive trends both monthly and annually suggests a systematic intensification of wind activity in the Darreh Dozdan River basin, which may be attributed to broader climatic changes or shifts in regional atmospheric circulation patterns over time. The results of this study indicate a statistically significant upward trend in monthly and annual wind speeds, which aligns with several regional and global investigations but also contrasts with others. For example, the findings are in agreement with the results of Ghaedi (2019) and Molaei and Lashkari (2020), who both reported significant increasing wind speed

trends in various parts of Iran, particularly in central and mountainous regions, where seasonal and annual analyses based on the Mann–Kendall test confirmed positive and significant Z values. These results suggest that, at least in parts of Iran, wind intensity has strengthened over recent decades. On a global scale, the observed trend partially corresponds with the findings of Kim and Paik (2015), who documented a recovery of surface wind speeds in South Korea after decades of decline, indicating that a reversal of the "stilling" phenomenon may be occurring in certain regions. However, other studies such as McVicar et al. (2012) and Vautard et al. (2010) have shown that, over the past 30–50 years, many parts of the Northern Hemisphere have experienced a marked reduction in near-surface wind speeds, often attributed to increased surface roughness, vegetation growth, and land-use changes. Additionally, Azorín-Molina et al. (2018) highlighted that part of the reported global decline in wind speed could be due to instrumental biases, particularly the aging of cup anemometers, suggesting that some stilling effects may be artificial. Therefore, while the increasing wind trend observed in this study is consistent with regional Iranian evidence and emerging signs of recovery in East Asia, it contrasts with the long-term global stilling trend observed in other mid-latitude regions, underscoring the spatial heterogeneity of wind speed variability and the importance of local climatic and surface conditions.

3.1.2. Sen's slope estimator

Table 2 presents the results of the wind speed trend analysis for the Darreh Dozdan River basin over the period 1998–2022 (25 years), conducted using Sen's slope estimator at both monthly and annual scales.

Table 2. Results of monthly and annual wind speed trends analysis using the Sen's slope estimator

Time series	Q_{med}	Q_{min}	Q_{max}	B	B_{min}	B_{max}
January	0.08	0.05	0.13	1.24	0.53	1.82
February	0.12	0.08	0.17	1.50	0.78	1.93
March	0.14	0.09	0.19	1.53	0.55	2.50
April	0.06	0.03	0.10	2.08	1.32	2.73
May	0.05	0.04	0.07	1.77	1.44	1.99
June	0.09	0.07	0.11	1.65	1.22	1.92
July	0.07	0.05	0.08	1.45	1.29	1.88
August	0.07	0.05	0.07	1.31	1.21	1.58
September	0.06	0.05	0.08	1.38	0.91	1.56
October	0.05	0.02	0.07	1.43	1.05	1.95
November	0.04	0.02	0.06	1.15	0.88	1.30
December	0.05	0.03	0.08	1.21	0.83	1.41
Annual	0.08	0.06	0.10	1.28	1.00	1.74

The Sen's slope analysis for the Darreh Dozdan River basin over the 1998–2022 period indicates a consistent and significant upward trend in wind speed for all months and annually. The median slopes (Q_{med}) range from 0.04 m/s per year in November, representing the smallest increase, to 0.14 m/s per year in March, reflecting the most pronounced strengthening of wind intensity. February (0.12 m/s per year) and March (0.14 m/s per year) show the highest monthly increases, indicating that late winter (February) and early spring (March) experience the fastest growth in wind speed. Conversely, May (0.05 m/s per year), October (0.05 m/s per year), and December (0.05 m/s per year) exhibit relatively low but still positive slopes, suggesting slower upward trends in late spring, autumn, and early winter, respectively. The annual Sen's slope value of 0.08 m/s per year confirms a steady long-term rise in wind speed across the region. These results demonstrate a persistent increase in wind activity, with seasonal variations showing more rapid growth during the transition from winter to spring and slower increases in late spring, autumn, and early winter. Figures 4 and 5 show the fitting of the Sen's line on the time series of monthly and annual wind speed data for the Darreh Dozdan River basin from 1998–2022 (25 years).

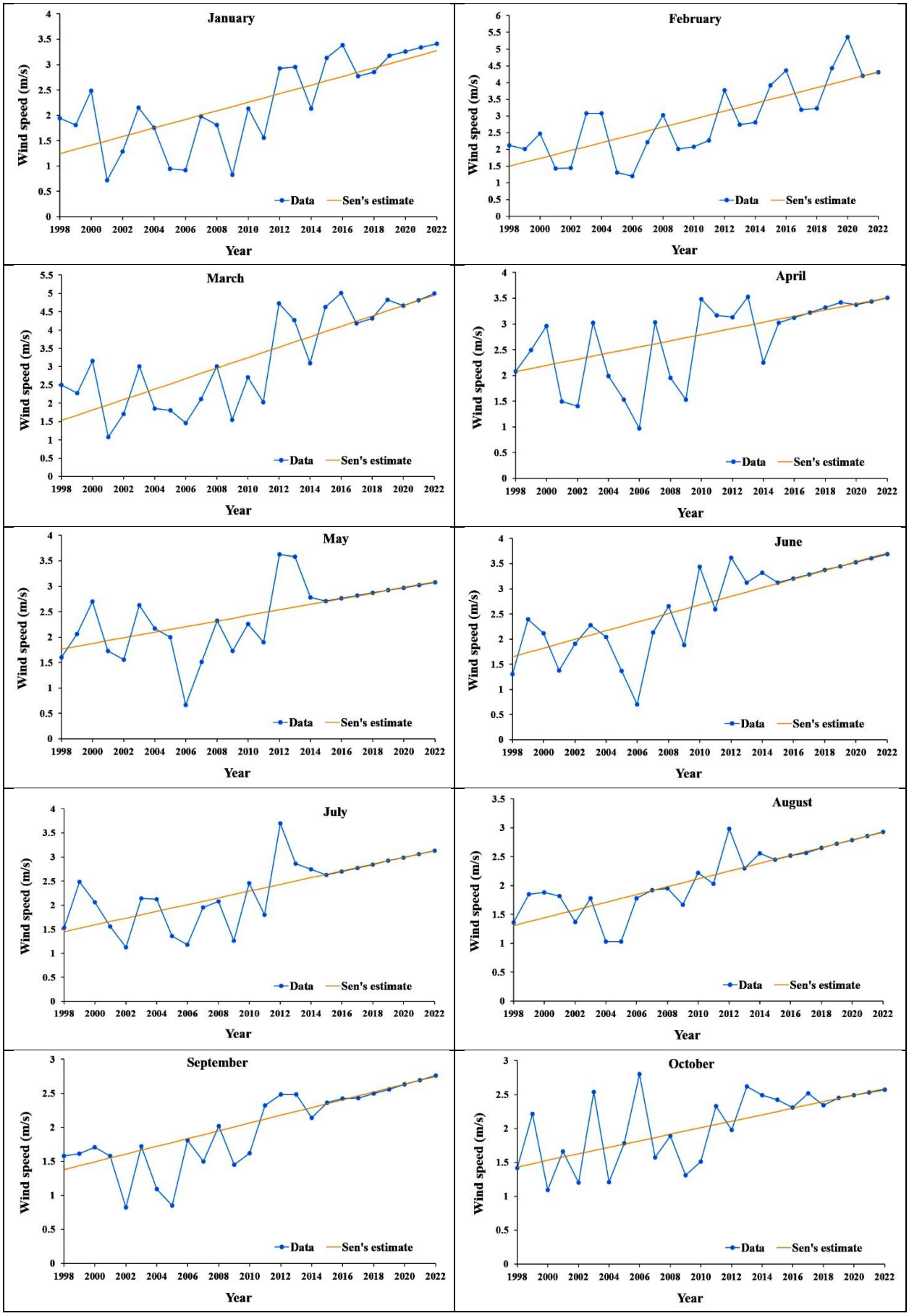
January
February
March
April
May
June
July
August
September
October
Wind speed (m/s)
Year
Data
Sen's estimate

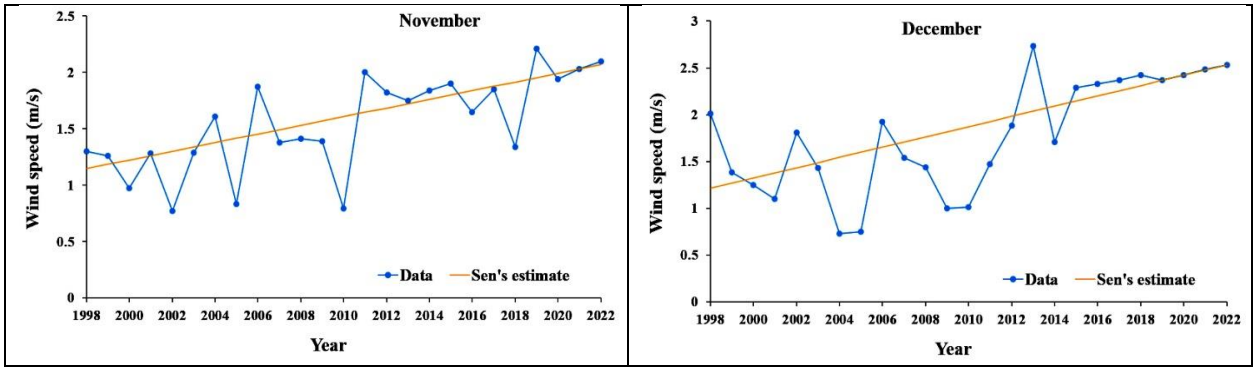

Figure 4. Fitting the Sen's line on the monthly wind speed time series data

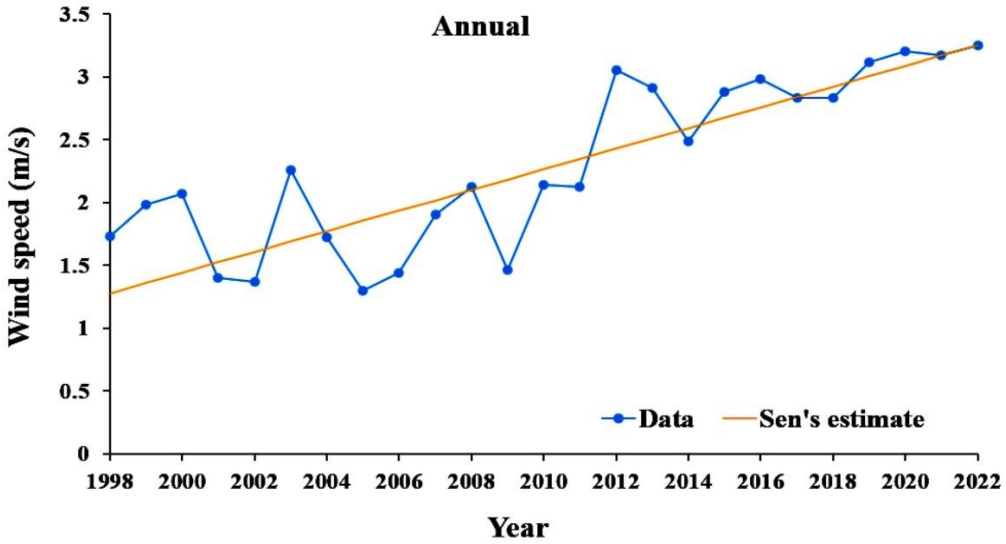

Figure 5. Fitting the Sen's line on the annual wind speed time series data

The comparison between the Mann–Kendall test and Sen's slope analysis for the Darreh Dozdan River basin wind speed data (1998–2022) reveals both consistencies and differences. Both methods confirm a statistically significant upward trend in wind speed across all months and annually, indicating a persistent increase in wind activity. However, the two approaches highlight different aspects of the trend. The Mann–Kendall Z values are highest in late summer and early autumn (August–September), reflecting strong statistical significance in these months, while the Sen's slope shows the largest annual increases in late winter and early spring (February–March), indicating that the greatest actual rise in wind speed occurs during this period. This discrepancy arises because Mann–Kendall measures trend significance without quantifying magnitude, whereas Sen's slope directly estimates the rate of change in m/s per year. Consequently, combining these two methods provides a comprehensive understanding of both the significance and the intensity of wind speed trends, showing that the region experiences steadily increasing wind speeds with seasonal variations in growth rates.

3.1.3. Pearson correlation coefficient

Table 3 presents the results of the wind speed trend analysis for the Darreh Dozdan River basin from 1998–2022 (25 years), using the Pearson correlation coefficient, on both monthly and annual scales.

Table 3. Results of wind speed trend analysis using the Pearson correlation coefficient

Time series	r	n	t	df	p-value	Significance level
January	0.73	25	5.17	23	0.00	Significant
February	0.77	25	5.78	23	0.00	Significant
March	0.79	25	6.27	23	0.00	Significant
April	0.64	25	3.96	23	0.00	Significant
May	0.63	25	3.87	23	0.00	Significant
June	0.81	25	6.74	23	0.00	Significant
July	0.71	25	4.86	23	0.00	Significant
August	0.84	25	7.44	23	0.00	Significant
September	0.82	25	6.98	23	0.00	Significant
October	0.64	25	3.98	23	0.00	Significant
November	0.70	25	4.76	23	0.00	Significant
December	0.70	25	4.64	23	0.00	Significant
Annual	0.84	25	7.46	23	0.00	Significant

The Pearson correlation analysis for the Darreh Dozdan River basin from 1998 to 2022 shows a statistically significant and positive relationship between wind speed and time at the 95% confidence level ($p < 0.05$) for all months and the annual series. The correlation coefficients (r) indicate that wind speed trends are strongly correlated ($0.6 < r < 0.8$) in nine months of the year, while highly correlated relationships ($r > 0.8$) are observed in June, August, September, and the annual scale. This pattern suggests that the increase in wind speed is particularly consistent and intense during the summer months, while remaining stable and notable throughout the rest of the year. A comparison between Pearson correlation coefficients and Mann–Kendall Z values shows a strong agreement in detecting statistically significant upward trends in wind speed across all months and annually at the 95% confidence level. The main similarity is that both methods confirm persistent long-term increases. Notably, the months June, August, and September show the highest values in both Mann–Kendall Z (4.27, 4.71, 4.86) and Pearson r (0.81, 0.84, 0.82), indicating a strong alignment between the monotonic trend and the linear correlation. Minor differences appear in July, which has a high Mann–Kendall Z (4.02) but a slightly lower Pearson r (0.71), reflecting a strong monotonic increase that is less strictly linear. This discrepancy arises because Mann–Kendall detects the significance of monotonic trends regardless of linearity, whereas Pearson emphasizes linear consistency, making months with smoother year-to-year increases appear stronger in correlation. Comparing Pearson correlation with Sen's slope highlights both agreement and differences. Both methods indicate positive and significant trends across all months. The highest Sen's slope values occur in February (0.12 m/s per year) and March (0.14 m/s per year), representing late winter and early spring, whereas the highest Pearson r values occur in June, August, and September, representing summer months with the most stable linear trend. The similarity is that both methods identify months with long-term wind speed increases, but the difference lies in what each emphasizes: Sen's slope measures the absolute rate of change, capturing periods with steep increases even amid interannual variability, while Pearson reflects linear stability, highlighting months where the increase is more consistent over time. Lower Sen's slope months (November 0.04, May 0.05, October 0.05) correspond reasonably well with lower Pearson r (0.63–0.70), confirming that both methods detect slower increases, albeit through different perspectives.

3.1.4. Regression analysis

Table 4 presents the results of the wind speed trend analysis for the Darreh Dozdan River basin from 1998–2022 (25 years), using linear regression analysis on both monthly and annual scales.

Table 4. Results of wind speed trend analysis using the linear regression analysis

Time series	a	b	p-value	Significance level
January	-171.96	0.09	0.00	Significant
February	-231.45	0.12	0.00	Significant
March	-284.21	0.14	0.00	Significant
April	-137.56	0.07	0.00	Significant
May	-118.31	0.06	0.00	Significant
June	-191.30	0.10	0.00	Significant
July	-133.56	0.07	0.00	Significant
August	-130.29	0.07	0.00	Significant
September	-127.99	0.06	0.00	Significant
October	-91.21	0.05	0.00	Significant
November	-79.83	0.04	0.00	Significant
December	-113.12	0.06	0.00	Significant
Annual	-150.65	0.08	0.00	Significant

The linear regression analysis of monthly and annual wind speed data for the Darreh Dozdan River basin during 1998–2022 indicates statistically significant positive trends for all months and the annual series at the 95% confidence level ($p < 0.05$). The slope coefficients (b) reveal seasonal variations in the rate of increase. The highest monthly increases are observed in March (0.14 m/s per year) and February (0.12 m/s per year), indicating the most pronounced rise in wind speed during late winter and early spring. Several months exhibit moderate increases, including January (0.09), June (0.10), April (0.07), July (0.07), and August (0.07), showing steady growth during winter and summer. Lower increases occur in May (0.06), September (0.06), December (0.06), October (0.05), and November (0.04), reflecting slower upward trends in late spring, early autumn, and late autumn. The annual slope of 0.08 m/s per year confirms a consistent long-term upward trend in wind speed across the region. Overall, the linear regression results indicate a systematic intensification of wind activity throughout the year, with strongest growth during late winter to early spring and weaker growth in autumn months, accurately reflecting the seasonal distribution of slope values. Figures 6 and 7 show the fitting of the linear regression on the time series of monthly and annual wind speed data for the Darreh Dozdan River basin from 1998–2022 (25 years).

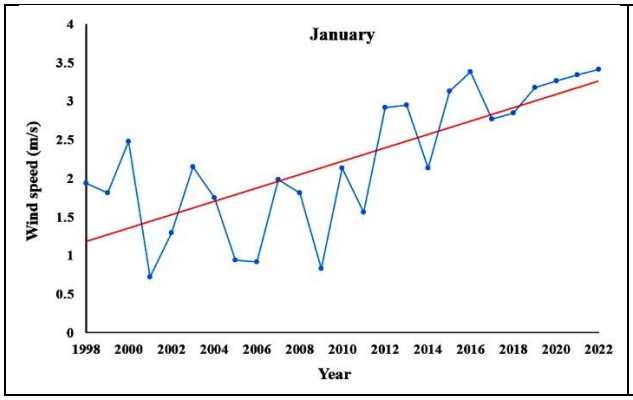

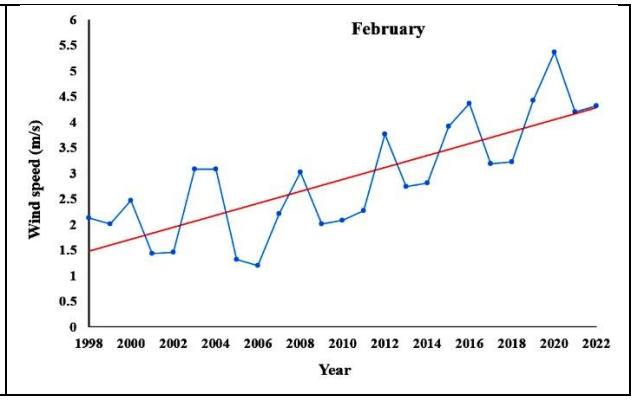

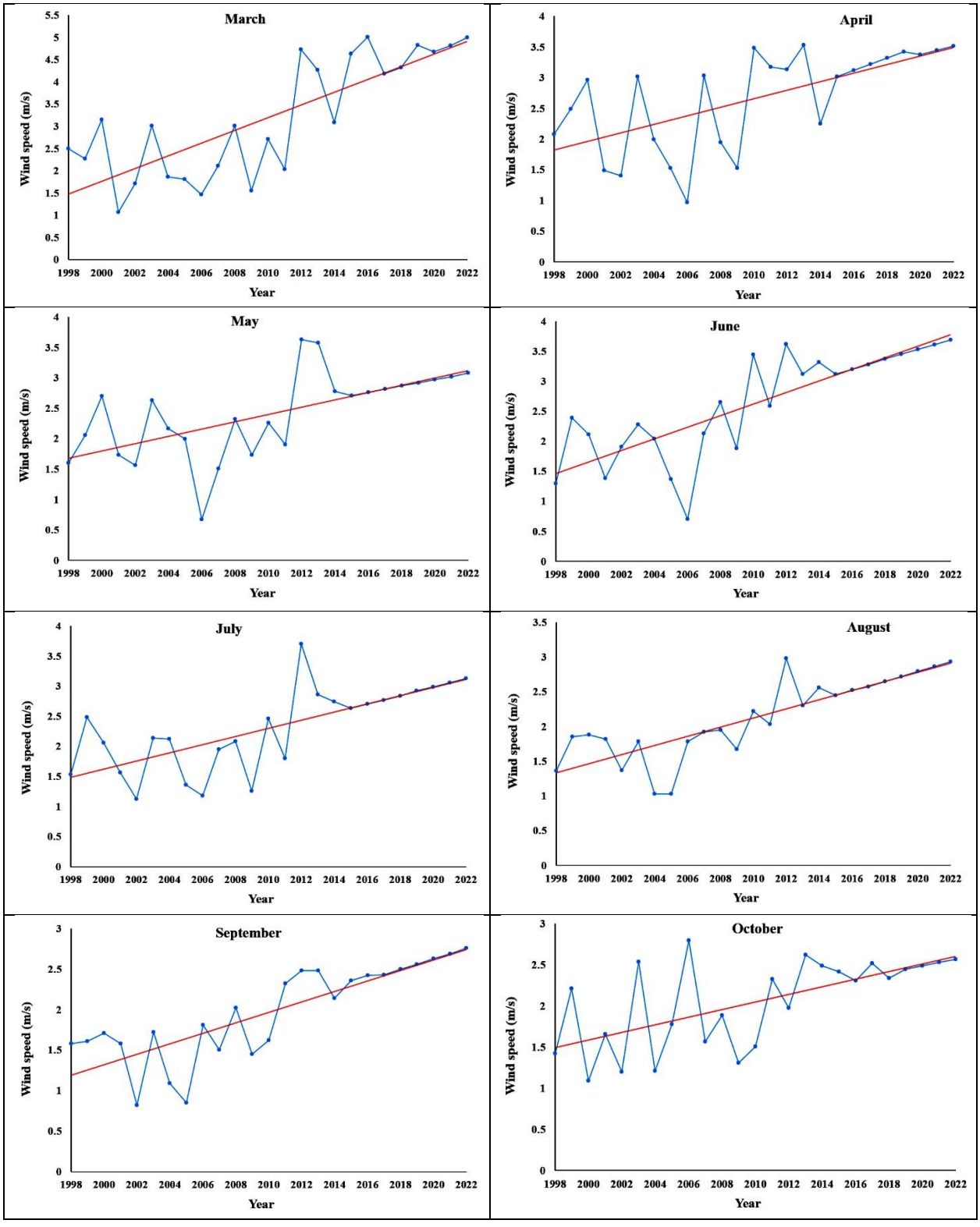
March
April
May
June
July
August
September
October
Wind speed (m/s)
Year

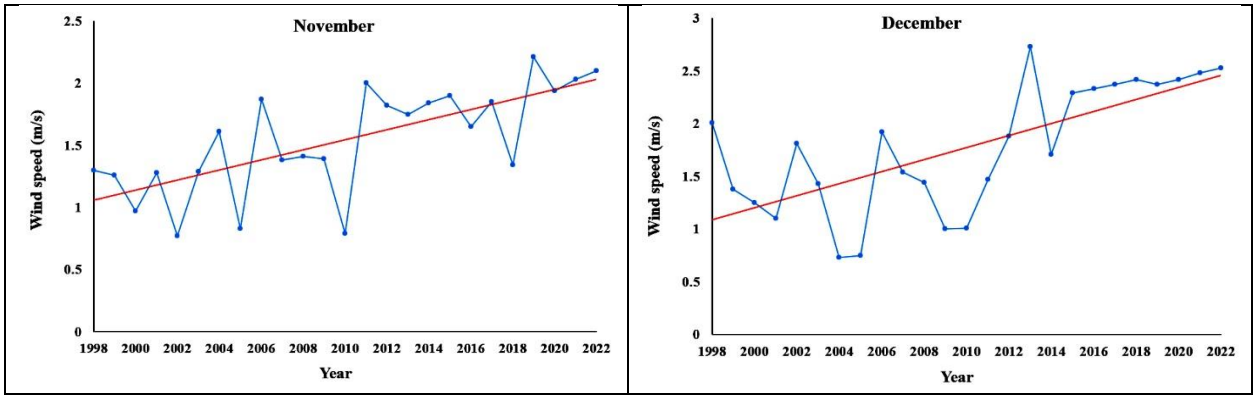

Figure 6. Fitting the linear regression on the monthly wind speed time series data

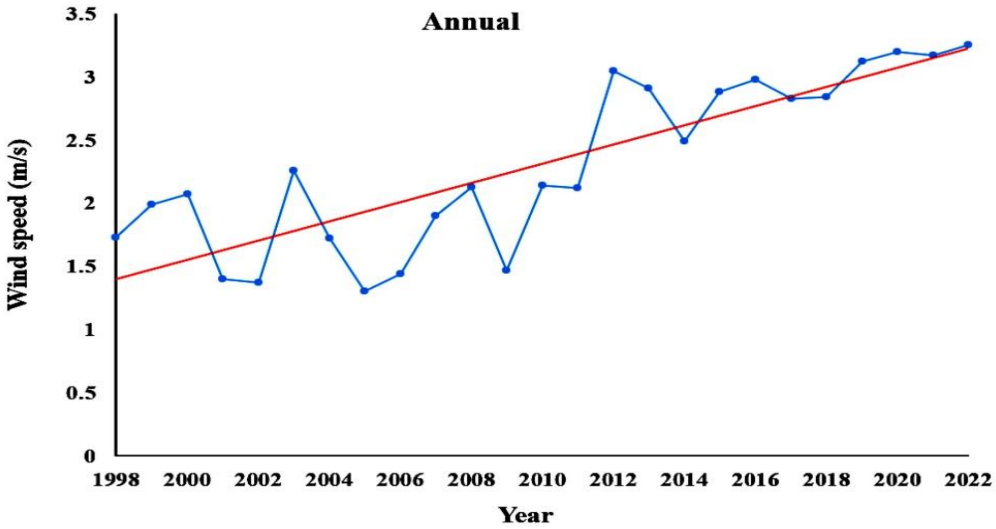

Figure 7. Fitting the linear regression on the annual wind speed time series data

The comparison of wind speed trends obtained from Mann–Kendall, Sen's slope, Pearson correlation, and linear regression reveals both strong agreements and minor discrepancies, reflecting the complementary nature of these methods. All four approaches consistently indicate a statistically significant upward trend in wind speed across all months and annually at the 95% confidence level, confirming the persistent long-term intensification of wind activity in the Darreh Dozdan River basin. Months with the highest increases generally align across methods. February and March show the largest slopes in Sen's slope (0.12–0.14 m/s per year) and linear regression (0.12–0.14 m/s per year), indicating rapid growth in late winter and early spring. Mann–Kendall and Pearson highlight the summer months of June, August, and September as periods with strong trends, reflecting both monotonic and linear increases. Low-growth months such as November and October are consistently identified across all methods. Minor discrepancies arise due to methodological focus. Mann–Kendall emphasizes the statistical significance of monotonic trends, highlighting August–September as peak months, even if the actual increase is moderate. Sen's slope and linear regression quantify the magnitude of change, with February–March showing the fastest growth. Pearson assesses linearity and consistency, so months with more stable year-to-year increases, particularly June, August, and September, exhibit higher correlation coefficients, even if their slope is slightly lower than February–March. This explains why the peak months differ between Pearson and regression despite both measuring linear trends: Pearson is influenced by stability and low interannual variability, whereas regression captures the absolute rate of change. Integrating these four methods provides a comprehensive understanding of wind speed trends, showing a persistent annual increase, with seasonal variations in both intensity and linearity, and

highlighting months of maximum growth and strongest trend stability.

4.Conclusion

This study analyzed monthly and annual wind speed trends in the Darreh Dozdan River Basin from 1998 to 2022 using four statistical methods: the Mann–Kendall test, Sen's slope estimator, Pearson correlation coefficient, and linear regression. The key results are presented below:

1. The Mann–Kendall test showed that all months had positive and statistically significant Z values greater than +1.96, confirming a persistent upward trend in wind speed. The strongest increases occurred in June, August, and September (Z = 4.27–4.86), reflecting intensified wind activity during the warmer months.
2. The Sen's slope and linear regression analyses revealed the largest increases in wind speed during February (0.12 m/s per year) and March (0.14 m/s per year), indicating that wind speeds rose most rapidly in late winter and early spring, while the annual results from both methods confirmed a steady increase in average wind speed of 0.08 m/s per year.
3. Pearson correlation coefficients showed significant positive relationships ($r > 0.6$ for all months), with the strongest correlations in June, August, and September ($r > 0.8$), confirming a highly consistent and stable upward trend during these months.
4. All four analytical methods converged on the conclusion that wind speed had increased in a statistically significant and persistent manner, differing only in which months exhibited the steepest or most stable growth, thereby providing a comprehensive and robust confirmation of wind intensification in the Darreh Dozdan River basin.

In the context of the Darreh Dozdan River basin, several recommendations can be made based on the findings of this study. First, it is suggested that future analyses employ Regional Climate Models (RCMs) instead of statistical models such as LARS-WG, which assume stationary wind patterns. The use of RCMs would enable the simulation of wind trends under actual climate change scenarios by capturing the influence of large-scale atmospheric circulation, topography, and regional variability. This approach would provide more reliable projections of future wind behavior in the basin. Second, future research should carefully select appropriate methods for estimating reference evapotranspiration. Many conventional approaches neglect the role of wind speed, which can introduce substantial errors in evapotranspiration calculations. Incorporating wind-sensitive methods will yield more accurate estimates of water requirements and contribute to improved irrigation scheduling and water resource management within the basin. Finally, it is recommended to assess the potential impacts of increasing wind speed on soil erosion processes in the Darreh Dozdan River basin. The identified upward trend in wind speed may intensify wind-driven soil loss, particularly in areas with sparse vegetation or loose surface materials. Future studies should integrate wind erosion modeling with field observations to identify vulnerable zones and develop effective land management and soil conservation strategies.

Statements and Declarations

Funding

The authors declare that no funds, grants, or other support were received during the preparation of this manuscript.

Data Availability

The data produced in this research are presented in the paper.

Conflict of Interest

The authors of this article declared no conflict of interest regarding the authorship or publication of this article.

Author contributions

Hedieh Ahmadpari: Data Collection, Data Analysis, Investigation, Methodology, Resources, Software, Writing – original draft, Writing – review and editing; Vitaly Khaustov: Conceptualization, Validation, Supervision, Writing – review and editing; Hamed Abbasali Nezhad: Conceptualization, Validation, Supervision, Writing – review and editing.

Declaration of AI Assistance

During the preparation of this work, the authors used the "https://chatgpt.com/" website for editing and language enhancement. The authors have thoroughly reviewed and revised the

content as necessary and assume full responsibility for the final manuscript.

References

1. Afrazfar, R., Abasalinezhad, H., & Simai, E. (2025). Evaluation and Monitoring of Meteorological Drought and Its Trend Analysis in Urmia County. Nivar, 49(130-131), 39-61. https://doi.org/10.30467/nivar.2025.511461.1326
2. Ahmadpari, H., & Khaustov, V. (2025a). Analyzing meteorological and hydrological droughts in the Darreh Dozdan River Basin through drought indices. Environment and Water Engineering, 11(2), 174-184. https://doi.org/10.22034/ewe.2025.506959.2004
3. Ahmadpari, H., & Khaustov, V. (2025b). Agricultural drought monitoring using meteorological indices in Darreh Dozdan Basin, Iran. Advances in Civil Engineering and Environmental Science, 2(2), 72-84. https://doi.org/10.22034/acees.2025.512324.1022
4. Ahmadpari, H., Hashemi Garmdareh, S. E., & Eskafi, M. (2018). Investigating the effect of soil organic matter on gypsum block calibration for measuring soil volumetric moisture content. Journal of Rainwater Catchment Systems, 6 (1), 11-20.
5. Ahmadpari, H., Khaustov, V., & Amini, A. (2025). Combined parametric and non-parametric assessment of relative humidity trends in a semi-arid river basin. Environment and Water Engineering, 11(4), 519-532. https://doi.org/10.22034/ewe.2025.538388.2048
6. Akçay, H., Eraslan, S., & Kara, M. (2022). Trend detection by innovative polygon trend analysis for winds and waves. Frontiers in Marine Science, 9, 930911. https://doi.org/10.3389/fmars.2022.930911
7. Amiri, M. J., Karbasi, A. R., Zoghi, M., & Sadat, M. (2015). Detection of climate changes by mann-kendall analysis and drought indexes (Case study: Agh Gol wetland). Journal of Environmental Studies, 41(3), 545-561. https://doi.org/10.22059/jes.2015.55896
8. Aschale, W., Tesfaye, A., & Gebremichael, B. (2023). Trend analysis and identification of the meteorological variables: A case study. Water, 15(3), 470. https://doi.org/10.3390/w15030470
9. Azorin-Molina, C., Asin, J., McVicar, T. R., Minola, L., Lopez-Moreno, J. I., Vicente-Serrano, S. M., & Chen, D. (2018). Evaluating anemometer drift: A statistical approach to correct biases in wind speed measurement. Atmospheric research, 203, 175-188. https://doi.org/10.1016/j.atmosres.2017.12.010
10. Balfour, N. J., & Ratnieks, F. L. W. (2025). Wind alters plant-pollinator community structure, bee foraging rate & movements between plants. Behavioral Ecology, 36(4), araf067. https://academic.oup.com/beheco/article/36/4/araf067/8162920
11. Berna-Escriche, C., Álvarez-Piñeiro, L., & Blanco, D. (2025). Forecasts Plus Assessments of Renewable Generation Performance, the Effect of Earth's Geographic Location on Solar and Wind Generation. Applied Sciences, 15(3), 1450. https://doi.org/10.3390/app15031450
12. Chen, Y., Guan, Y., Shao, G., & Zhang, D. (2016). Investigating trends in streamflow and precipitation in Huangfuchuan Basin with wavelet analysis and the Mann-Kendall test. Water, 8(3), 1-32. https://doi.org/10.3390/w8030077
13. Deng, K., Azorin-Molina, C., Minola, L., Zhang, G., & Chen, D. (2021). Global near-surface wind speed changes over the last decades revealed by reanalyses and CMIP6 model simulations. Journal of Climate, 34(6), 2313–2333. https://doi.org/10.1175/JCLI-D-20-0337.1
14. FAO. (2023). The State of Food Security and Nutrition in the World 2023: Urbanization, agrifood systems transformation and healthy diets across the rural–urban continuum. Food and Agriculture Organization of the United Nations (FAO). https://doi.org/10.4060/cc3017en
15. Fu, J., Gong, Y., Zheng, W., Zou, J., Zhang, M., Zhang, Z., & Qin, J. (2022). Spatial temporal variations of terrestrial evapotranspiration across China from 2000

to 2019. Science of The Total Environment, 825, 153951. https://doi.org/10.1016/j.scitotenv.2022.153951
16. Ghaedi, S. (2019). Wind Speed Trends in Iran. Desert Management, 7(13), 15-28. https://doi.org/10.22034/jdmal.2019.36529
17. Gocic, M., & Trajkovic, S. (2013). Analysis of changes in meteorological variables using Mann-Kendall and Sen's slope estimator statistical tests in Serbia. Global and planetary change, 100, 172-182. https://doi.org/10.1016/j.gloplacha.2012.10.014
18. Gutiérrez Hernández, J., López Márquez, A., & Ramírez Castillo, J. (2024). Robust trend analysis in environmental remote sensing: Applications of Mann–Kendall and Sen's slope estimator. Remote Sensing, 16(20), 3886. https://doi.org/10.3390/rs16203886
19. Hahmann, A. N., García-Santiago, O., & Peña, A. (2022). Current and future wind energy resources in the North Sea according to CMIP6. Wind Energy Science, 7, 2373–2391. https://doi.org/10.5194/wes-7-2373-2022
20. Hejazizadeh, Z., Akbari, M., Sasanpour, F., Hosseini, A., & Mohammadi, N. (2022). Investigating the effects of climate change on torrential rains in Tehran province. Water and Soil Management and Modelling, 2(2), 87-105. https://doi.org/10.22098/mmws.2022.9958.1075
21. Intergovernmental Panel on Climate Change (IPCC). (2022). Climate Change 2022: Impacts, Adaptation and Vulnerability. Contribution of Working Group II to the Sixth Assessment Report of the Intergovernmental Panel on Climate Change. Cambridge University Press. https://doi.org/10.1017/9781009325844
22. Jiang, Y., & Sun, W. (2025). Day-Ahead electricity price prediction and error correction method based on feature construction–singular spectrum analysis–long short-term memory. Energies, 18(4), 1-22. https://doi.org/10.3390/en18040919
23. Kara, T., & Şahin, A. D. (2023). Implications of Climate Change on Wind Energy Potential. Sustainability, 15(20), 14822. https://doi.org/10.3390/su152014822
24. Keskin, M. Z., Abu Arra, A., Akca, S., & Şişman, E. (2025). Actual and potential trend analysis under climate change using risk Sen's Slope (RSS) in Western Black Sea Basin in Türkiye. International Journal of Climatology, 45(1), e8703. https://doi.org/10.1002/joc.8703
25. Kim, J., & Paik, K. (2015). Recent recovery of surface wind speed after decadal decrease: a focus on South Korea. Climate Dynamics, 45(5), 1699-1712. https://doi.org/10.1007/s00382-015-2546-9
26. Kleidon, A., Messori, G., Baidya Roy, S., Didenkulova, I., & Zeng, N. (2023). Editorial: Global warming is due to an enhanced greenhouse effect, and anthropogenic heat emissions currently play a negligible role at the global scale. Earth System Dynamics, 14, 241–242. https://doi.org/10.5194/esd-14-241-2023
27. Kwak, S. (2023). Are only p-values less than 0.05 significant? A p-value greater than 0.05 is also significant! Journal of Lipid and Atherosclerosis, 12(2), 89–95. https://doi.org/10.12997/jla.2023.12.2.89
28. Liu, L., & Xu, Z. X. (2016). Regionalization of precipitation and the spatiotemporal distribution of extreme precipitation in southwestern China. Natural Hazards, 80, 1195-1211. https://doi.org/10.1007/s11069-015-2018-x
29. Liu, S., Xie, Y., Fang, H., Du, H., & Xu, P. (2022). Trend Test for Hydrological and Climatic Time Series Considering the Interaction of Trend and Autocorrelations. Water, 14(19), 3006. https://doi.org/10.3390/w14193006
30. Luo, F., Xiao, H., Gao, J., Ma, Y., Li, X., Li, J., Miri, A., Cao, Q., & Xin, Z. (2022). Microclimate and wind regime of three typical landscapes in the Northeastern Ulan Buh Desert. Frontiers in Environmental Science, 10, 939739. https://doi.org/10.3389/fenvs.2022.939739
31. Markwitz, P., Knohl, A., & Siebicke, L. (2020). Evapotranspiration over

agroforestry sites in Germany. Biogeosciences, 17, 5183–5199. https://doi.org/10.5194/bg-17-5183-2020

32. McVicar, T. R., Roderick, M. L., Donohue, R. J., Li, L. T., Van Niel, T. G., Thomas, A., ... & Dinpashoh, Y. (2012). Global review and synthesis of trends in observed terrestrial near-surface wind speeds: Implications for evaporation. Journal of Hydrology, 416, 182-205. https://doi.org/10.1016/j.jhydrol.2011.10.024
33. Mincu, A., Popescu, I., & Ionescu, D. (2025). Evaluation of Temporal Changes in Evapotranspiration and Crop Water Requirements in the Context of Changing Climate: Case Study of the Northern Bucharest–Ilfov Development Region, Romania. Agricultural Water Management, 295, 108875. https://doi.org/10.1016/j.agwat.2025.108875
34. Mirabbasi, R., Ahmadi, F., & Jhajharia, D. (2020). Comparison of parametric and non parametric methods for trend identification in groundwater levels in Sirjan plain aquifer, Iran. Hydrology Research, 51(6), 1455–1470. https://doi.org/10.2166/nh.2020.041
35. Mokari, M., & Abbasnia, M. (2020). Trends analysis of maximum temperature by using Mann-Kendall and Spearman Tests in various regions of Iran. Nivar, 44(108-109), 31-44. https://doi.org/10.30467/nivar.2020.211885.1143
36. Molaei, A., & Lashkari, H. (2020). Investigation of wind speed trend changes in central Iran using ECMWF Reanalysis data. Physical Geography Research, 52(3), 481-498. https://doi.org/10.22059/jphgr.2020.295406.1007476
37. Muhlbauer, A., Spichtinger, P., & Lohmann, U. (2009). Application and comparison of robust linear regression methods for trend estimation. Journal of Applied Meteorology and Climatology, 48(9), 1961-1970. https://doi.org/10.1175/2009jamc1851.1
38. Nguyen, H. M., Ouillon, S., & Vu, V. D. (2022). Sea level variation and trend analysis by comparing Mann–Kendall test and innovative trend analysis in front of the Red River Delta, Vietnam (1961–2020). Water, 14(11), 1709. https://doi.org/10.3390/w14111709
39. Obilor, E. I. & Amadi, E. C. (2018). Test for Significance of Pearson's Correlation Coefficient. International Journal of Innovative Mathematics, Statistics & Energy Policies, 6(1), 11-23
40. Owasa, H. A., & Fall, A. F. (2024). Food Security in Developing Countries: Factors and Mitigation. American Journal of Climate Change, 13, 391–405. https://doi.org/10.4236/ajcc.2024.133018
41. Park, C., Shin, S. W., Cha, D. H., Min, S. K., Byun, Y. H., Kim, J. U., & Choi, Y. (2024). Impact of global warming on wind power potential over East Asia. Renewable and Sustainable Energy Reviews, 203, 114747. https://doi.org/10.1016/j.rser.2024.114747
42. Qin, X., Li, Y., Wang, H., & Zhang, L. (2025). The effects of wind erosion depending on cropping system and tillage method in a semi-arid region. Agriculture, 15(2), 387. https://www.mdpi.com/2073-4395/15/2/387
43. Rahman, M. M., Rahman, M. S., & Alam, M. S. (2022). Impact of climate change on agricultural production; Issues, challenges, and opportunities in Asia. Frontiers in Plant Science, 13, 925548. https://doi.org/10.3389/fpls.2022.925548
44. Rasheed, A., & Ullah, S. (2023). Interactions between wind patterns, agricultural productivity, and climate change impacts. Agricultural Systems, 208, 103656. https://doi.org/10.1016/j.agsy.2023.103656
45. Shi, W., Dong, Z., Chen, G., Bai, Z., & Ma, F. (2022). Spatial and temporal variation of the near-surface wind environment in the Sahara Desert, North Africa. Frontiers in Earth Science, 10, 789800. https://doi.org/10.3389/feart.2021.789800
46. Siddiqui, A., Al-Ansari, T., & Kholief, M. (2025). High-resolution projection of wind

energy in the Eastern Mediterranean and Middle East summer. Climatic Change, 171, 45. https://doi.org/10.1007/s10584-025-03951-2

47. Smith, J., Adepoju, R., & Mensah, K. (2022). The impact of climate variability and change on food security in Sub Saharan Africa: Perspective from Panel Data Analysis. Sustainability, 14(2), 759. https://doi.org/10.3390/su14020759
48. Tanikawa, M., & Hashimoto, S. (2022). Impacts of Global Climate Change on Agricultural Production: A Comprehensive Review. Agriculture, 12(9), 1234. https://doi.org/10.3390/agriculture12091234
49. Thenmozhi, M., & Kottiswaran, S. V. (2016). Analysis of rainfall trend using Mann-Kendall test and the Sen's slope estimator in Udumalpet of Tirupur district in Tamil Nadu. International journal of agricultural science and research, 6(2), 131-138.
50. Totaro, V., Gioia, A., & Iacobellis, V. (2020). Numerical investigation on the power of parametric and nonparametric tests for trend detection in annual maximum series. Hydrology and Earth System Sciences, 24, 473–491. https://doi.org/10.5194/hess-24-473-2020
51. Vautard, R., Cattiaux, J., Yiou, P., Thépaut, J. N., & Ciais, P. (2010). Northern Hemisphere atmospheric stilling partly attributed to an increase in surface roughness. Nature geoscience, 3(11), 756-761. https://doi.org/10.1038/ngeo979
52. Wang, X., Liu, Y., & Chen, H. (2024). Projected changes in global atmospheric circulation and surface wind patterns under future climate scenarios. Environmental Research Letters, 19(4), 045007. https://doi.org/10.1088/1748-9326/ad1a64
53. Wanniarachchi, S., & Sarukkalige, R. (2022). A Review on Evapotranspiration Estimation in Agricultural Water Management: Past, Present, and Future. Hydrology, 9(7), 123. https://doi.org/10.3390/hydrology9070123
54. Yılmaz, A., & Kara, M. (2024). Statistical analysis of wind speed data with different distributions: Bitlis, Türkiye. Turkish Journal of Nature and Science, 13(4), 5–10. https://doi.org/10.46810/tdfd.1440444
55. Zhang, P., Chen, G., & Ming, Y. (2021). Quantifying the mechanisms of atmospheric circulation response to greenhouse gas increases in a forcing–feedback framework. Journal of Climate, 34(17), 7005–7022.
56. Zhao, X., Wu, Y., Su, J., & Gou, J. (2023). Surface wind speed changes and their potential impact on wind energy resources across China during 1961–2021. GeoHealth, 7(8), e2023GH000861. https://doi.org/10.1029/2023GH000861